The β4 Integrin Interactor p27$^{BBP/eIF6}$ Is an Essential Nuclear Matrix Protein Involved in 60S Ribosomal Subunit Assembly

Francesca Sanvito,*‡ Simonetta Piatti,§ Antonello Villa,*‖ Mario Bossi,*‖ Giovanna Lucchini,§ Pier Carlo Marchisio,*¶ and Stefano Biffo*

*DIBIT, Department of Biological and Technological Research, and ‡Department of Pathology, San Raffaele Scientific Institute, 20132 Milano, Italy; §Dipartimento di Genetica e di Biologia dei Microrganismi, University of Milano, 20133 Milano, Italy; ‖Department of Pharmacology, University of Milano and CNR Center, 20129 Milano, Italy; and ¶Department of Biomedical Sciences and Human Oncology, University of Torino School of Medicine, 10126 Torino, Italy

Abstract. p27$^{BBP/eIF6}$ is an evolutionarily conserved protein that was originally identified as p27^{BBP}, an interactor of the cytoplasmic domain of integrin β4 and, independently, as the putative translation initiation factor eIF6. To establish the in vivo function of p27$^{BBP/eIF6}$, its topographical distribution was investigated in mammalian cells and the effects of disrupting the corresponding gene was studied in the budding yeast, *Saccharomyces cerevisiae*. In epithelial cells containing β4 integrin, p27$^{BBP/eIF6}$ is present in the cytoplasm and enriched at hemidesmosomes with a pattern similar to that of β4 integrin. Surprisingly, in the absence and in the presence of the β4 integrin subunit, p27$^{BBP/eIF6}$ is in the nucleolus and associated with the nuclear matrix. Deletion of the *IIH S. cerevisiae* gene, encoding the yeast p27$^{BBP/eIF6}$ homologue, is lethal, and depletion of the corresponding gene product is associated with a dramatic decrease of the level of free ribosomal 60S subunit. Furthermore, human p27$^{BBP/eIF6}$ can rescue the lethal effect of the *iih*Δ yeast mutation. The data obtained in vivo suggest an evolutionarily conserved function of p27$^{BBP/eIF6}$ in ribosome biogenesis or assembly rather than in translation. A further function related to the β4 integrin subunit may have evolved specifically in higher eukaryotic cells.

Key words: epithelial cells • yeast • nucleolus • hemidesmosomes • intermediate filaments

Integrins are heterodimeric receptors formed by the assembly of one α and one β transmembrane subunit. 16 α and 8 β subunits heterodimerize to produce >20 receptors that are differentially expressed in a wide variety of tissues. Most integrins bind components of the extracellular matrix and can organize the cytoskeleton through their cytoplasmic domain (for review see Hynes, 1992). Moreover, integrins are involved in the control of cell growth, apoptosis, and differentiation through the recruiting of several signal transduction and adaptor molecules (for review see Clark and Brugge, 1995; Giancotti, 1997; Howe et al., 1998). The steadily increasing role of integrins in the organization of cellular metabolic processes has recently encompassed the process of protein synthesis. Indeed, clustering of some integrin subunits at points of focal adhesion results in the relocation of mRNA and ribosomes to focal adhesion contacts (Chicurel et al., 1998). Although the molecular mechanisms of this process are unknown, a picture in which most biochemical processes are spatially regulated, with integrins playing a major role, has emerged.

The integrin subunit β4 associates with α6 to form a multivalent laminin receptor present at high levels in most epithelia. Its ligand engagement correlates with PI3 kinase activation (Shaw et al., 1997) and recruitment of the shc and grb2 adaptors (Mainiero et al., 1995). In addition, in squamous and transitional epithelia, β4 is required for the formation of hemidesmosomes, specialized structures providing firm mechanical links between basal lamina and the intermediate filament cytoskeleton (for review see Giancotti, 1996). Loss of function of β4 both in human and mice results in hemidesmosome disruption, blistering, and perinatal death (Vidal et al., 1995; Dowling et al., 1996; van der Neut et al., 1996).

Mutations in the functional cytodomain of β4 result in an inability to translocate into hemidesmosomes and be targeted to the intermediate filament cytoskeleton (Spinardi et al., 1993; Niessen et al., 1997) accompanied by lethal forms of the blistering disease junctional *epidermolysis bullosa* associated with *pyloric atresia* (Vidal et al., 1995). These and other data strongly indicate that the

F. Sanvito and S. Piatti contributed equally to this work.

Address correspondence to Stefano Biffo, Lab. Istologia Molecolare DIBIT, San Raffaele Scientific Institute, V. Olgettina 58, 20132 Milano, Italy. Tel.: 39-22-643-4857. Fax: 39-22-643-4855. E-mail: s.biffo@hsr.it

cytodomain of β4 exerts its function through the interaction with cytoplasmic molecules led us to search for protein interactors of the β4 cytodomain. Through an extensive yeast two hybrid analysis, a previously unknown peptide named $p27^{BBP}$ (BBP for beta4 binding protein)[1] that binds the β4 cytodomain was discovered. $p27^{BBP}$ directly binds, in vitro and in vivo, a 300–amino acid long stretch of β4 integrin cytodomain, a region required for targeting β4 to the hemidesmosomes and to the intermediate filament cytoskeleton as determined by genetic studies. In addition, $p27^{BBP}$ was found to be present at high levels in the submembrane region of epithelial cells containing β4. Finally, the biochemical association of $p27^{BBP}$ with keratin intermediate filaments, suggested that $p27^{BBP}$ might be the molecular link between β4 and the cytoskeleton (Biffo et al., 1997). The precise ultrastructural localization of $p27^{BBP}$, in in vivo hemidesmosomes was not yet defined.

The finding that $p27^{BBP}$ homologues exist both in yeast and *Drosophila*, in which β4 integrin homologues are absent (Biffo et al., 1997) suggested that $p27^{BBP}$ might also have a β4-independent function. Consistently, the cloning of a human cDNA encoding a protein named eIF6 (identical to $p27^{BBP}$) was almost concomitantly obtained by Si et al. (1997). The biological assay used to clone eIF6 was based on its in vitro ability to inhibit the association between the 40S and the 60S ribosomal subunits, and was not related to integrin function. On the basis of its in vitro determined properties, it was suggested that eIF6 might act as a translation initiation factor. The cloning and sequencing of eIF6 unequivocally indicate that eIF6 and $p27^{BBP}$ are the same protein (Biffo et al., 1997; Si et al., 1997). Much more recently, eIF6/$p27^{BBP}$ has also been identified by another group as a gene induced in mast cells by allergic reaction (Cho et al., 1998). To acknowledge the independent identification of $p27^{BBP}$ and eIF6, the protein will be denoted as $p27^{BBP/eIF6}$ throughout this work.

Both studies left a set of unresolved questions: (a) Which is the precise cellular localization of $p27^{BBP/eIF6}$ and is it modulated by the presence of β4 integrin?; (b) Is the association of $p27^{BBP/eIF6}$ with the intermediate filament cytoskeleton a unique feature of cells that contain β4?; (c) Is $p27^{BBP/eIF6}$ present in hemidesmosomes?; and (d) Which is the general, evolutionarily conserved, function of $p27^{BBP/eIF6}$? To address these questions, we used integrated approaches. First, the fine localization of $p27^{BBP/eIF6}$ was studied in cell lines, either containing β4 integrin or not. Our studies show that $p27^{BBP/eIF6}$ is a nuclear matrix-associated protein present in the nucleolus of all cells analyzed and enriched at the basal membrane of β4 expressing epithelial cells. Second, the function of $p27^{BBP/eIF6}$ was addressed in *Saccharomyces cerevisiae* by constructing and characterizing a null mutant. The yeast $p27^{BBP/eIF6}$ homologue is essential for cell viability and its depletion results in an abnormal ribosomal profile, with a dramatic reduction of the levels of free 60S ribosomal subunits. Taken together these data indicate that the conserved role of $p27^{BBP/eIF6}$ is linked to 60S ribosome subunit metabolism, and that this process may be linked to the nuclear matrix. In higher organisms, novel functions of $p27^{BBP/eIF6}$ may have appeared that link this molecule to epithelial adhesion.

1. *Abbreviations used in this paper:* BBP, beta4 binding protein; ECL, chemiluminescence detection system; eIF, eukaryotic (translation) initiation factor; HA, hemagglutinin; IIH, integrin interacting homologue.

Materials and Methods

Antibodies and Cell Lines

The rabbit polyclonal antiserum against the COOH-terminal peptide of $p27^{BBP/eIF6}$ (NH_2-CTIATSMRDSLIDSLT-COOH) was tested for its specificity by Western blotting and immunoprecipitation both on the recombinant protein and on cellular lysates (Biffo et al., 1997). Integrin β4 was detected with the rat mAb3E1 (10 μg/ml; Chemicon International, Inc.), or with the mouse mAb AA3 (Kajiji et al., 1989) at 10 μg/ml (gift of Vito Quaranta, Scripps Research Institute, La Jolla, CA). The human autoantibodies against fibrillarin (Ochs and Smetana, 1991) were a generous gift of Robert Ochs (Scripps Research Institute) and were diluted 1:300. Cytokeratins were detected either with mouse monoclonal anticytokeratin 8:18, IgG2a (Diagnostika) at 1:200, or with mouse monoclonal anticytokeratin 7/17 IgG1, according to the manufacturer's protocol (C46; Euro-Diagnostica). Secondary antibodies were rhodamine- and fluorescein-tagged swine anti–rabbit IgGs (1:50; DAKO Corp.), rhodamine-tagged goat anti–human IgGs (10 μg/ml; Chemicon International, Inc.), rhodamine-tagged goat anti–mouse IgGs (7.5 μg/ml; Molecular Probes Europe) and fluorescein-tagged goat anti–mouse IgGs (1:50; Antibodies Inc.). In control experiments, primary antibodies were replaced by preimmune sera or irrelevant mAbs. In addition, the $p27^{BBP/eIF6}$ antiserum was preadsorbed with the peptide used for its generation (1 μM, overnight, 4°C), or with the bacterially produced human recombinant full length protein (at 10 μg/ml, 2 h at 4°C) purified by ion exchange chromatography.

The cell lines and primary cells used in this study, as well as the conditions for their propagation, are described in the American Type Culture Collection cell line catalogue or in the references between parentheses. They are as follows: mouse NIH/3T3 fibroblasts, human A431 epidermoid carcinoma, human HeLa epitheloid carcinoma, human pancreatic carcinoma FG2 (Kajiji et al., 1989), human Jurkat T cells, transformed human keratinocytes HaCat (Boukamp et al., 1988), human insulinoma cells Rin2A (Rouiller et al., 1990), and human neuroblastoma SK-N-MC. The 804G rat epithelial cell line clone A was a gift of F. Giancotti (Memorial Sloan-Kettering Cancer Center, New York) and has been described in Spinardi et al. (1993).

Mouse resting splenocytes, human fibroblasts from the umbilical cord, and *Xenopus* oocytes were gifts of A. Cabibbo, E. Bianchi, and E. Pannese (all at DIBIT, Milano, Italy) and were obtained by standard procedures.

Actinomycin Treatment

Cells were treated with actinomycin D (Boehringer Mannheim GmbH) at the final concentration of 5 μg/ml for 1, 4, and 12 h, washed, and fixed as described. In some experiments cells were allowed to recover after treatment by switching them to their normal medium.

Electron Microscopy on Human Amnion

Human fresh amniotic membrane (obtained immediately upon delivery from the Department of Obstetrics, San Raffaele Hospital, Milano, Italy) was dissected and pieces of tissue were fixed with 4% paraformaldehyde and 0.25% glutaraldehyde in 125 mM sodium phosphate buffer, pH 7.4, for 45 min at 4°C. The samples were infiltrated with polyvinylpyrrolidone and frozen in a 3:1 (vol/vol) mixture of propane and isopentane cooled with liquid nitrogen. Ultrathin cryosections (50–100 nm thick) were obtained using an Ultracut ultramicrotome equipped with a Reichert FC4 cryosectioning apparatus. The cryosections were processed as described in Villa et al. (1993) using the rabbit anti-$p27^{BBP/eIF6}$ antiserum and the mouse monoclonal anticytokeratin 7/17 IgG1. Cryosections were examined in an electron microscope (Hitachi H-7000).

Western Blot Analysis

All samples were denatured before loading in Laemmli buffer (Laemmli, 1970) and run on denaturing 12% SDS–acrylamide gel, transferred to Immobilon P membranes (Millipore Corp.), and blotted with the rabbit

p27$^{BBP/eIF6}$ antiserum at 1:1,000 dilution as previously described (Biffo et al., 1997). In the control of the fractionation experiment, a mouse monoclonal anticytokeratin 8/18 IgG2a at 1:200 was used. Detection was always performed by the commercially available chemiluminescence detection system (ECL) technique (Nycomed Amersham).

Extraction of Nuclear Matrix and Ribosomal Proteins

Intermediate filaments/nuclear matrix filaments fractions were prepared exactly according to He et al. (1990). Briefly, all the soluble proteins, the nonintermediate filament cytoskeleton, DNA associated proteins, and proteins loosely associated with the nuclear matrix proteins were removed by sequential washes in buffers (Triton X-100, 250 mM ammonium sulphate, DNase I, and 2 M NaCl). At the end of this procedure, a cytoplasmic and nuclear intermediate filament network containing keratins, lamins, and intermediate filament-associated proteins was left. The efficiency of the extraction was routinely controlled by DNA staining, or by immunostaining for keratins.

Preparation of ribosomes was performed through established procedures and exactly as described in Madjar (1994). 804G clone A cell line monolayer was washed and scraped with cold PBS. The pellet was resuspended in cold buffer A (0.25 M sucrose, 25 mM KCl, 5 mM $MgCl_2$, 50 mM Tris-HCl, pH 7.4), stirred slowly with a vortex, while adding NP-40 to a final concentration of 0.7%, and kept on ice for 10 min. The suspension was centrifuged at 750 *g* for 10 min at 4°C and the resulting pellet containing nuclei and insoluble proteins was resuspended in Laemmli buffer for biochemical analysis. The supernatant was centrifuged at 12,500 *g*, 10 min at 4°C and the resulting pellet containing mitochondria was resuspended in Laemmli buffer. The low-speed supernatant was added to 0.32 vol of buffer C (0.25 M sucrose, 2 M KCl, 5 mM $MgCl_2$, 50 mM Tris-HCl, pH 7.4), layered on top of a 1 M sucrose cushion, and ultracentrifuged (TL100; Beckman Instruments, Inc.) at 245,000 *g*, 2 h at 4°C. The high-speed pellet containing ribosomal proteins was resuspended in Laemmli buffer. The high-speed supernatant was precipitated with cold 10% TCA, for 45 min on ice, centrifuged at 14,000 rpm at 4°C, and resuspended in Laemmli buffer for biochemical analysis.

Indirect Immunofluorescence and Immunocytochemistry

Immunofluorescence was performed as previously reported (Marchisio et al., 1991). In brief, the following was performed: cell monolayers were fixed in 3% paraformaldehyde in PBS, pH 7.6, containing 2% sucrose for 10 min at room temperature; permeabilized in Hepes–Triton X-100 buffer for 5 min at 4°C (20 mM Hepes, 300 mM sucrose, 50 mM NaCl, 3 mM $MgCl_2$, 0.5% Triton X-100, pH 7.4); and blocked with 5% BSA in PBS for 30 min at room temperature. Next, the cells were incubated in primary antibodies (diluted in 5% BSA in PBS) for 2 h at room temperature, washed in 0.2% BSA in PBS, and treated with secondary antibodies diluted in PBS. Staining for F-actin was performed with 200 nM fluorescein-labeled phalloidin (Sigma Chemical Co.) for 20 min at 37°C in the dark and with 2 μg/ml DNA counterstaining (Hoechst 33342; Sigma Chemical Co.). Once mounted in Mowiol 4-88 (Hoechst AG), coverslips were analyzed with a confocal microscope (MRC-1024; Bio-Rad Laboratories) equipped with a krypton/argon laser. To reduce bleed through, double-label confocal images (XY and XZ sections) were acquired sequentially. Micrographs were taken using either a Focus Imagecorder Plus (Focus Graphics Inc.) on Kodak film or a Professional color Point II dye sublimation printer (Seiko). Stained cells were observed in parallel with a Zeiss Axiophot microscope equipped for epifluorescence and a 63× planapochromatic lens; pictures were taken on Kodak T-MAX 400 films exposed at 1000 ISO and developed at 1600 ISO in T-MAX developer for 10 min at 20°C.

In some experiments, p27$^{BBP/eIF6}$ was revealed by immunoperoxidase labeling using the avidin–biotin amplification method (ABC Kit Vectastain; Vector Labs Inc.). Briefly, after incubation with the primary antiserum cell monolayers were washed and treated with a goat anti–rabbit biotin-conjugated antibody for 30 min at room temperature, followed by the preformed avidin–biotin complex (ABC). The staining was revealed by horseradish peroxidase and 3,3′-diaminobenzidine as chromogen (Bio-Genex Labs).

Electron Microscopy on Extracted Cells

FG2 cells were extracted to reveal the nuclear matrix as described above and fixed with fresh 3.7% paraformaldehyde in digestion buffer for 30 min at 4°C. They were washed once in digestion buffer, once in TBS-1 (10 mM Tris-HCl, pH 7.7, 150 mM NaCl, 3 mM KCl, 1.5 mM $MgCl_2$, 0.05% Tween 20, 0.1% BSA, 0.2% glycine), and blocked in 5% BSA in TBS-1 for 30 min at room temperature. The cells were incubated in rabbit p27$^{BBP/eIF6}$ antiserum, 1:200 in 5% BSA in TBS-1 rocking overnight at 4°C. After this incubation, they were sequentially washed in TBS-1, blocked with 5% BSA in TBS-1, 10 min at room temperature, and incubated with 5-nm gold bead-conjugated goat anti–rabbit antibody (Jackson ImmunoResearch Laboratories, Inc.), 1:40 in TBS-2 (20 mM Tris-HCl, pH 8.2, 140 mM NaCl, 0.1% BSA) rocking for 1 h at room temperature. Cells were washed in TBS-1, postfixed in 2.5% glutaraldehyde in 0.1 M cacodylate buffer, pH 7.4, and centrifuged at low speed (600 *g* for 5 min). The cell pellets were included in diethylene glycol distearate as described by Nickerson et al. (1994). Resinless sections were examined in a Hitachi H-7000 electron microscope.

Database Searches

Homology searches were performed with the Blast programs available through http://www.ncbi.nlm.nih.gov, or by the alerting system of EMBL (http://www.bork.embl-heidelberg.de/Alerting). The accession number of the sequences retrieved are: *Homo sapiens*, Y11435; *S. cerevisiae*, Z49919; *Caenorhabditis elegans*, Z99709; *Arabidopsis thaliana*, AC003000; *Methanococcus jannaschii*, U67463; *S. acidocaldarius*, P38619; *Methanobacterium thermoautotrophicum*, AE000920; *P. bomkoshii*, AB009481; and *Archaeoglobus fulgidus*, AE000961. The alignment was created using the CLUSTAL W algorithm (Thompson et al., 1994). The phylogram of the aligned proteins were produced with the GROWTREE program in GCG with the Jukes-Cantor distance matrix and neighbor-joining method.

Yeast Strains and Media

All strains used are derivatives of W303 (*MATa*, *ade2-1*, *trp1-1*, *leu2-3*, *112*, *his3-11,15*, *ura3*, *can1–100*). Cells were grown in YEP medium (1% yeast extract, 2% bactopeptone, 50 μg/liter adenine) supplemented with either 2% glucose (YEPD) or 2% raffinose and 1% galactose (YEPRG). Transformants carrying the *kanMX4* cassette were selected on YEPD plates containing 400 μg/ml G418 (US Biological).

Plasmid Construction and Genetic Manipulations of Yeast Strains

Standard techniques were used for genetic crosses (Rose et al., 1990) and DNA manipulations (Sambrook et al., 1989). The yeast integrin interacting homologue (*IIH1*) gene was cloned by PCR using as a template the genomic DNA of strain W303 and oligonucleotides oSP44 (5′CAGAATAGTCGGAGAAGCGGAC3′) and oSP45 (5′GTAAGGTGCAAGATCAGACAAAG 3′). To construct a *IIH1* chromosomal deletion (*iih1::kanMX4*), the heterologous *kanMX4* cassette was amplified by PCR using plasmid pFA6a-*kanMX4* (Wach et al., 1994) as a template and oligonucleotides oSP43 (5′CGCATACAACTGTAAACAGACTTGAGGAAGGAGGGGAATCCCCTCAGGAGATCGATGAATTCGAGCTC-G3′) and oSP46 (5′GCCTCATCCCTCGTTCTTATAGTATAATTACAAGAAGCAATACGACAGCGTACGCTGCAGGTCGAC3′) as primers. The amplification product contained the *kanMX4* cassette flanked by *IIH1* sequences (underlined in the oligonucleotide sequences) and was used to transform the diploid strain W303. G418-resistant transformants were shown by PCR analysis to be heterozygous for the replacement of most of the *IIH1* chromosomal ORF with the *kanMX4* cassette. By sporulation and tetrad analysis of one of these transformants (ySP478), *iih1::kanMX4* segregants were shown to be inviable, since all tetrads contained only two viable spores that were always G418 sensitive.

To construct the *GAL–IIH1* fusion (pSP43), the *IIH1* XbaI/SspI fragment was cloned in XbaI (SalI) of a Yiplac211-derived plasmid (Gietz and Sugino, 1988) that carried the BamHI–EcoRI *GAL1-10* promoter fragment (c2139). To construct the *GAL-Hsp27*$^{BBP/eIF6}$ fusion (pSP40), a PCR fragment containing a hemagglutinin (HA)-tagged version of *Hsp27*$^{BBP/eIF6}$ was amplified using as a template the pSG5-p27 expression plasmid in which the entire open reading frame of human *p27*$^{BBP/eIF6}$ gene was cloned in frame with a 10–amino acid HA tag in the NH_2 terminus (the original vector is described in Green et al., 1988, the HA-modified vector was a gift of V. Zappavigna, DIBIT). The oligonucleotides YSTAG (5′CGGAATTCAACAATAATGTACCCATACGAGCTTCCA3′) and YASTAG2 (5′CGGAATTCCTAGGTGAGGCTGTCAATGAGGGA3′), where the sequences of the human gene and of the HA tag are underlined

were used as primers. The obtained PCR product was cut with EcoRI and cloned in the EcoRI site of c2139. Both *GAL-IIH1* and *GAL-Hsp27*$^{BBP/eIF6}$ fusions were integrated at the *ura3* locus of ySP478 by cutting pSP43 and pSP40 with ApaI before transformation. As a result, strains ySP650 (*GAL-IIH1* single copy), ySP653 (*GAL-Hsp27*$^{BBP/eIF6}$ single copy), and ySP652 (*GAL-Hsp27*$^{BBP/eIF6}$ multiple copies), respectively were generated. The copy number of the integrated plasmids was checked by Southern analysis. Strain ySP661 (*MATa*, *iih1::kanMX4*, and *ura3::URA3::GAL-IIH1*) was obtained after sporulation and tetrad dissection of ySP650, whereas ySP664 (*MATa*, *iih1::kanMX4*, and *ura3::URA3::GAL-Hsp27*$^{BBP/eIF6}$) was obtained after sporulation and tetrad dissection of ySP653.

Polysome and Western Blot Analysis of Ribosomal Fractions

Polyribosome preparation and polysome analysis were done exactly according to Foiani et al. (1991). Briefly, cell cultures of W303 (wt), ySP661 (*iih1*Δ, *GAL-IIH1*), and ySP664 (*iih1*Δ, *GAL-HSp27*$^{BBP/eIF6}$) were grown in YEPRG medium and shifted to YEPD at time 0 to repress the *GAL* promoter. Yeast extracts were prepared from 300 ml of cell culture at OD = 0.5–1 (Foiani et al., 1991), layered on a 7–47% sucrose gradient in 50 mM Tris-acetate, pH 7.0, 50 mM NH_4Cl, 12 mM $MgCl_2$, and 1 mM dithiothreitol and centrifuged at 4°C in a SW41 Beckman rotor for 2 h at 39,000 rpm. Gradient analysis was performed with a gradient collector with continuous monitoring at A_{254}.

For protein analysis, the collected fractions were precipitated with TCA to a final concentration of 10% and left on ice for 30 min. Fractions were centrifuged at 15,000 *g*, for 15 min at 4°C, and resuspended in Laemmli buffer. Equal amounts of extracts were run on denaturing 12% acrylamide gels and blotted as described above.

Results

p27$^{BBP/eIF6}$ Is Present in all Cell Lines, at Early Developmental Stages and Is Associated with the Cytoskeleton

It was previously observed that p27$^{BBP/eIF6}$ mRNA was highly expressed during mouse embryonic development and that highly conserved homologues were present in the unicellular organism *S. cerevisiae* (Biffo et al., 1997). These data suggested that p27$^{BBP/eIF6}$ might have a general role in cellular processes that is not limited to epithelial cells expressing β4 integrin only. To test this hypothesis, the expression of p27$^{BBP/eIF6}$ was first measured by Western blot analysis with a polyclonal antiserum directed against the COOH terminus of p27$^{BBP/eIF6}$ on total protein lysates from immortalized cell lines of various origin (see Materials and Methods for original references). So far, p27$^{BBP/eIF6}$ has been detected in all cell lines analyzed. Fig. 1 (left) shows the levels of p27$^{BBP/eIF6}$ in the immortalized cell lines NIH/3T3 (nontransformed mouse fibroblasts), Jurkat (human T cells), SK-N-MC (human neuroblastoma), A431, HeLa, HaCaT, and FG2 (transformed human epithelial cell lines), and Rin2A (human insulinoma). Constitutive expression of p27$^{BBP/eIF6}$ was also detected in two out of two primary cultures tested, respectively, human primary fibroblasts, and mouse resting splenocytes.

It was previously observed that p27$^{BBP/eIF6}$ mRNA was abundant during embryonic development and declined in the adult, where it was mainly retained in epithelial tissues (Biffo et al., 1997). To test the hypothesis that p27$^{BBP/eIF6}$ protein may be present already at early phases of development, its onset was studied in embryos. The protein was found to be expressed from the earliest developmental stage and later on. Fig. 1 (right) shows p27$^{BBP/eIF6}$ in the

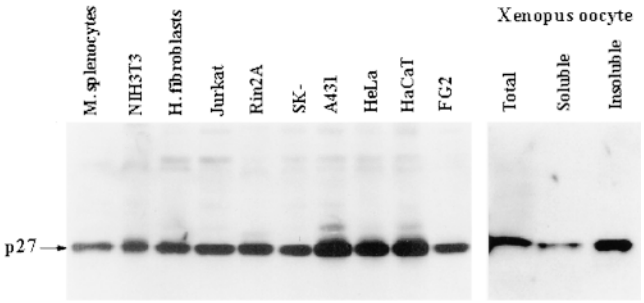

Figure 1. p27$^{BBP/eIF6}$ is present in all cell lines, and in a cytoskeletal associated pool. (Left) 30 μg of total protein extracts from established cell lines and primary cultures were run on 12% acrylamide gels, transferred on immobilon-P membranes and blotted with the p27$^{BBP/eIF6}$ antiserum, followed by ECL detection. The arrow points at the p27$^{BBP/eIF6}$ band. The cell lines were mouse NIH/3T3 fibroblasts, human A431 epidermoid carcinoma, human HeLa epitheloid carcinoma, human pancreatic carcinoma FG2, human Jurkat T cells, transformed human keratinocytes HaCaT, human insulinoma cells Rin2A, and human neuroblastoma SK-N-MC. Primary cultures were mouse resting splenocytes and human fibroblasts. (Right) p27$^{BBP/eIF6}$ in *Xenopus* oocytes extracted either in Laemmli buffer (total), or according to the nuclear matrix/intermediate filaments procedure of He et al. (1990, see Materials and Methods). The lane marked soluble contains cytosolic proteins extracted with an isotonic Triton X-100 buffer. The lane marked insoluble contains nuclear matrix/intermediate filament-associated proteins left after sequential extraction with ammonium sulphate, nuclease, and high salt.

Xenopus egg, between fertilization and the beginning of segmentation. Comparable results were obtained in mice. As previously observed for p27$^{BBP/eIF6}$ mRNA, in the adult, high levels of p27$^{BBP/eIF6}$ protein were retained mostly in epithelial tissues, and testis (not shown).

In epithelial cells containing β4 integrin, ~50% of p27$^{BBP/eIF6}$ was associated with the intermediate filament cytoskeleton (Biffo et al., 1997). The association of p27$^{BBP/eIF6}$ with the cytoskeleton was analyzed in cell lines not containing β4 integrin. For this purpose, cells were first extracted with detergent containing buffers (Materials and Methods) and the various fractions were analyzed by Western blot. Part of p27$^{BBP/eIF6}$ was always found in the cytoskeletal fraction. However, the extent of the association varied according to the cell line (not shown). Fig. 1 (right) shows the results of the fractionation experiments in *Xenopus* eggs, where at least half of p27$^{BBP/eIF6}$ was found to be resistant to detergent extraction and associated with the cytoskeleton.

Nucleolar Localization of p27$^{BBP/eIF6}$

The topographical distribution of p27$^{BBP/eIF6}$ was studied in detail by immunofluorescence, immunocytochemistry, and electron microscopy. To summarize our findings, as shown in Figs. 2–4, p27$^{BBP/eIF6}$ was present in the nucleus, with a clear nucleolar pattern. The nucleolar staining of p27$^{BBP/eIF6}$ was present in all the organisms analyzed so far (from worms to humans) and in all cell lines. In addition, in some cell lines containing β4 integrin, p27$^{BBP/eIF6}$ was

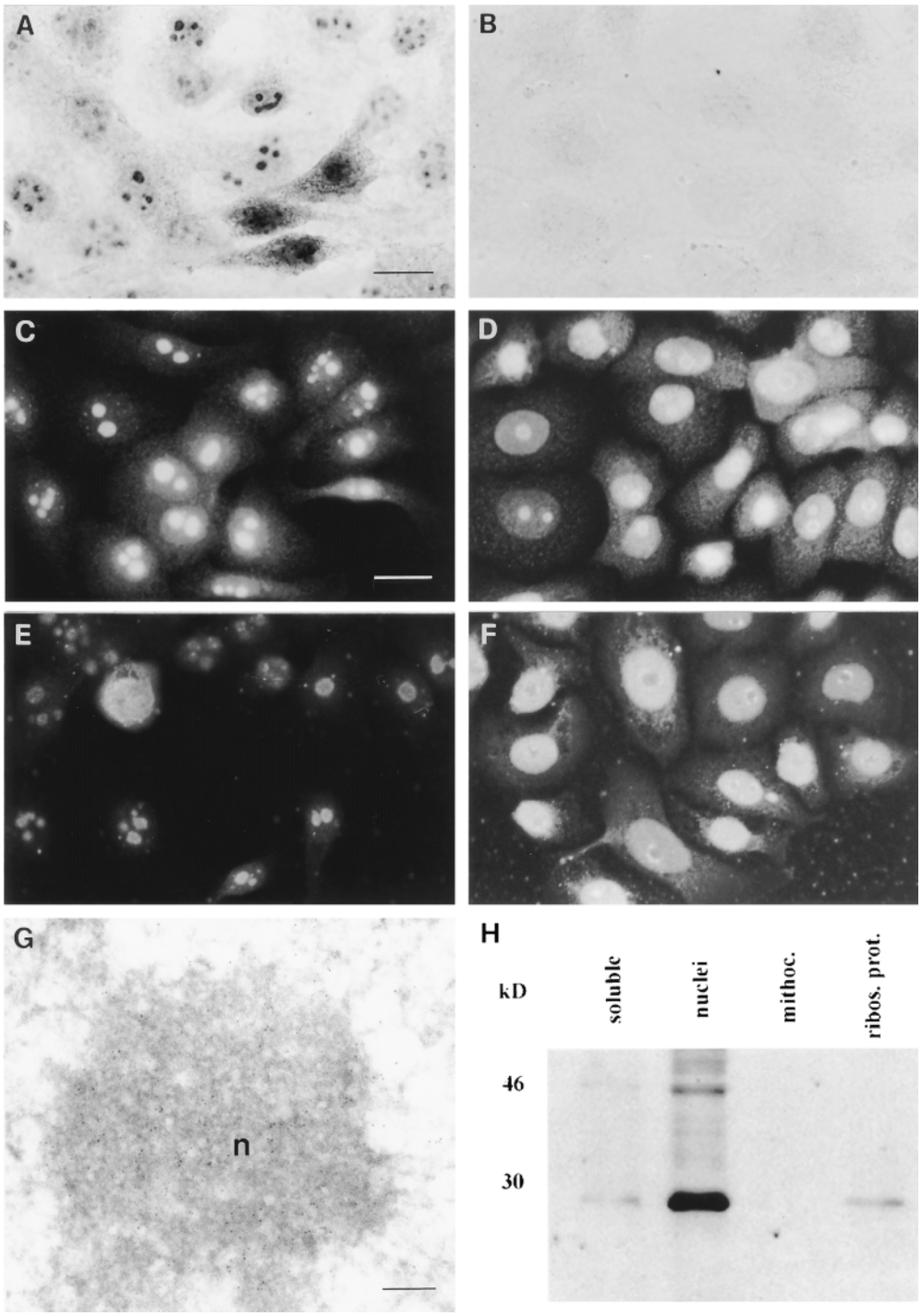

Figure 2. $p27^{BBP/eIF6}$ is always present in the nucleolus. The experiments were performed on the FG2 cell line. Identical results are obtained with all cell lines. FG2 cells were stained with the specific $p27^{BBP/eIF6}$ antiserum, revealed by immunoperoxidase (A and B) or immunofluorescence (C and D) and with a human antiserum recognizing the nucleolar marker fibrillarin (nucleoantiserum; E and F) followed by immunofluorescence. A strong $p27^{BBP/eIF6}$ nuclear staining, as well as a weaker cytoplasmic staining are visible in A. The staining was completely eliminated by pre-adsorption of the antiserum with the pure recombinant $p27^{BBP/eIF6}$ protein. (B) The immunofluorescence pattern of $p27^{BBP/eIF6}$ in normal untreated cells is shown where one to three intensely labeled dots are present in nuclei (C). By comparison, the pattern of the nucleolar antigen fibrillarin is shown (E); the large labeled cell in the middle is in early prophase. The effects of treatment with actinomycin D for 4 h on the pattern of both $p27^{BBP/eIF6}$ (D) and fibrillarin (F) are shown. This treatment results in the loss of the nucleolus: note that both $p27^{BBP/eIF6}$ and fibrillarin largely redistribute within the nucleus. Bar (A–F), 5 μm. Immunoelectron microscopy localization of $p27^{BBP/eIF6}$ within the nucleolus of epithelial cells (G). Cells were sequentially treated with $p27^{BBP/eIF6}$ antiserum followed by 5-nm gold-conjugated secondary antibodies. Note the high number of gold particles scattered throughout the nucleolus (n). Bar, 0.1 μm. Proteins from the 804G cell line were separated in the following fractions: soluble, nuclear (also containing highly insoluble intermediate filament-associated proteins), mitochondrial, and ribosomal as described in the Materials and Methods.

clearly evident in the cytoplasm (see Fig. 5). All the immunoreactivity described is specific, since both the nuclear and the cytoplasmic staining could be routinely abolished by preincubating the antiserum with either the peptide used for immunization or with the recombinant protein (Fig. 2, A and B). In addition, a similar nucleolus-enriched staining pattern could be seen on NIH/3T3 fibroblasts transfected with a HA-tagged version of $p27^{BBP/eIF6}$, followed by immunofluorescence with a mouse anti-HA mAb (not shown).

The nuclear staining of $p27^{BBP/eIF6}$ and its dynamic features will be described using the FG2 cell line as a model. In the interphase nucleus, $p27^{BBP/eIF6}$ was clearly concentrated in the nucleolus (Fig. 2, A and C). This pattern was similar to the one obtained with an antiserum recognizing the nucleolar protein, fibrillarin (Fig. 2 E). The nucleolar

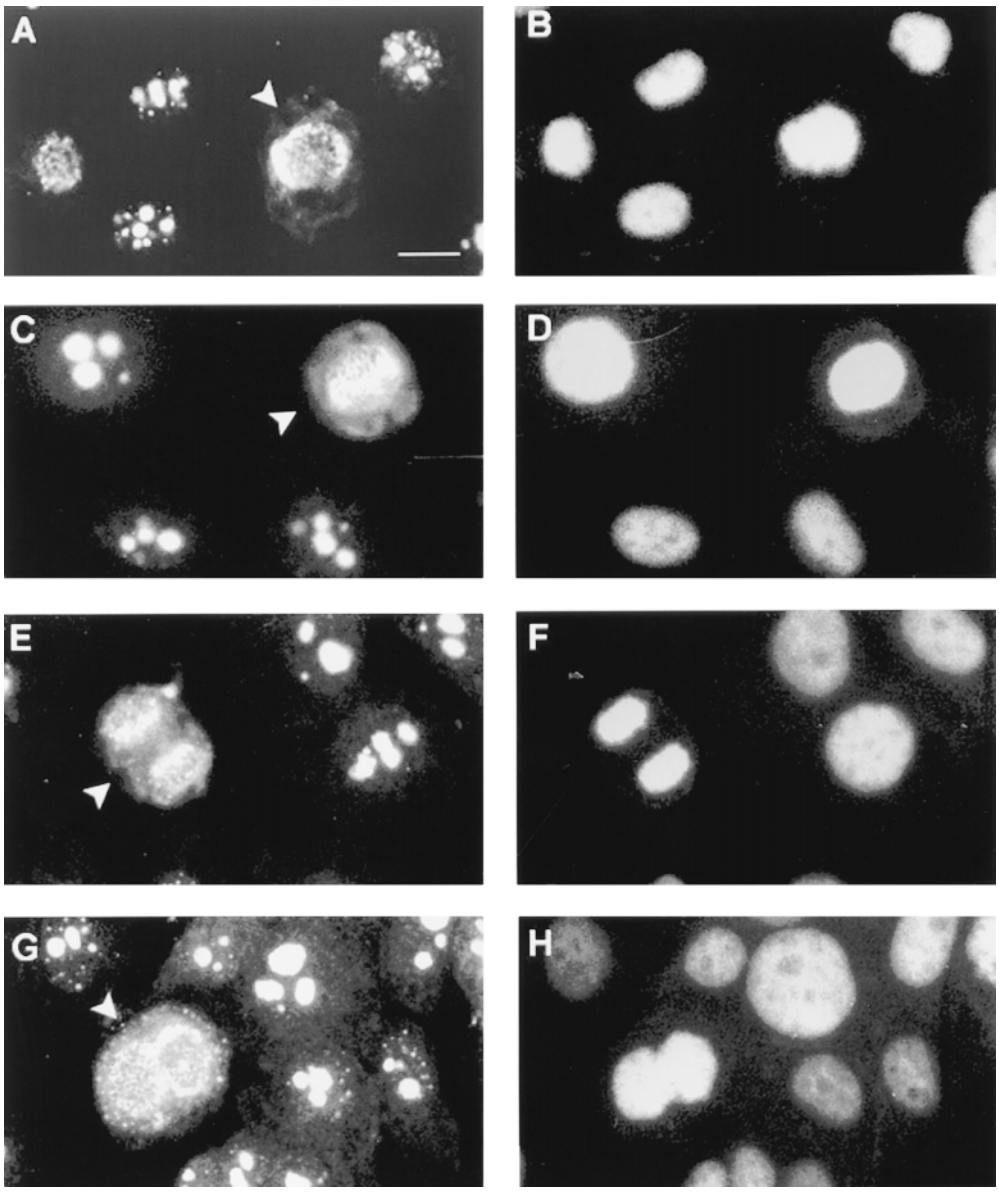

Figure 3. $p27^{BBP/eIF6}$ becomes associated with condensed chromosomes during mitosis. FG2 cells were stained using the rabbit anti–$p27^{BBP/eIF6}$ antiserum. The arrowheads point to cells at specific phases of mitosis: prophase (B), metaphase (D), anaphase (F), and telophase (H) as detected with Hoechst dye. In early prophase (A), the nuclear membrane dissolves and $p27^{BBP/eIF6}$ appears diffuse. During metaphase $p27^{BBP/eIF6}$ staining concentrates in the condensed chromosomes, at the metaphasic plate (C); then in anaphase it associates with the segregating chromatids (E). In G, with the formation of the membranes of the two nuclei, $p27^{BBP/eIF6}$ appears again diffuse in and around the nucleus, before concentrating again in the nucleolus (all surrounding cells). Bar, 5 μm.

colocalization was supported by double immunofluorescence studies with fibrillarin and $p27^{BBP/eIF6}$ (not shown).

To establish whether $p27^{BBP/eIF6}$ was dynamically associated with the nucleolus, epithelial cells were treated with low doses of actinomycin D and $p27^{BBP/eIF6}$ localization was analyzed after 1, 4, and 12 h. This treatment caused the collapse of the nucleolus and the redistribution of nucleolar-associated proteins (Schofer et al., 1996). In actinomycin D–treated cells, both $p27^{BBP/eIF6}$ (Fig. 2 D) and the nucleolar antigen, fibrillarin (Fig. 2 F), reversibly weakened their association with the nucleolus and became mostly diffuse in the cell's nucleus. Importantly, no effect on $p27^{BBP/eIF6}$ localization was seen when cells were treated with the protein synthesis inhibitors, cycloheximide and puromycin (not shown). Nucleolar localization of $p27^{BBP/eIF6}$ was confirmed by immunoelectron microscopy, using the anti-$p27^{BBP/eIF6}$ antiserum, followed by 5-nm gold-labeled secondary antibodies. 5-nm gold beads were strongly concentrated within the nucleolus (Fig. 2 G).

Next, we tested whether $p27^{BBP/eIF6}$ was stably associated with ribosomal proteins in the cytoplasm of the 804G-clone A epithelial cell line. For this purpose, ribosomes and ribosomal proteins were separated from all of the following: mitochondria, nuclear matrix/intermediate filaments, and soluble proteins. Afterwards, the different fractions were tested for the presence of $p27^{BBP/eIF6}$ by Western blot analysis. As shown in Fig. 2 H, most of the protein was present in the nuclear matrix/intermediate filament cytoskeleton fraction. A faint band was associated with the ribosomal fraction.

$p27^{BBP/eIF6}$ Redistributes during Mitosis

The strong nucleolar-associated pattern of $p27^{BBP/eIF6}$ was visible in all cell lines during interphase, as well as in various normal and neoplastic tissues (Sanvito, F., manuscript in preparation). Therefore, it was expected that during mitosis, when the nucleolus disappears, the protein would be redistributed. Indeed, during cell division $p27^{BBP/eIF6}$ dra-

matically changed its topographical pattern. At prophase, the immunoreactivity tended to become more dispersed at first. Later, it became associated with the periphery of condensed chromosomes (Fig. 3, A and B). At metaphase, $p27^{BBP/eIF6}$ was enriched in the central mass of chromatin formed by the condensed chromosomes of the metaphasic plate (Fig. 3, C and D) and this pattern was even more noted at anaphase (Fig. 3, E and F). With the onset of telophase and the reappearance of the nucleolar organization, $p27^{BBP/eIF6}$ first scattered and then regained its association with the nucleolus (Fig. 3, G and H). The redistribution of $p27^{BBP/eIF6}$ during the mitotic phases was not associated with its proteolytic degradation. Furthermore, no obvious physical association of $p27^{BBP/eIF6}$ with tubulin was observed (not shown). A similar redistribution was observed for some nucleolar antigens, chromosome passengers, which redistribute around chromosomes during mitosis (Earnshaw and Bernat, 1991), as well as for some nuclear matrix-associated antigens, whose immunoreactivity become more dispersed during mitosis (Nickerson et al., 1992).

$p27^{BBP/eIF6}$ Is Associated with the Nuclear Matrix

To investigate whether the nucleolar $p27^{BBP/eIF6}$ was associated with the nuclear matrix, FG2 cells were extracted with a sequential treatment by means of detergents, DNase, RNase, and high salts (He et al., 1990), and then analyzed by immunofluorescence and electron microscopy. This treatment removed >90% of the proteins, and 95% of the DNA. In addition, the treatment uncovered a nuclear matrix consisting of a nuclear lamina connected to the cytoplasmic intermediate filaments and of an internal meshwork of polymorphic fibers connecting the lamina to masses within the nucleus. In conditions that lead to the complete loss of DNA (Fig. 4 D), the $p27^{BBP/eIF6}$ staining, associated with the nucleolus was clearly retained (Fig. 4, C–E). Also, the nuclear staining of $p27^{BBP/eIF6}$ was unaffected after digestion of residual RNA with RNase (not shown).

To establish whether the residual staining of $p27^{BBP/eIF6}$ was present in specific structures, extracted cells were examined by immunoelectron microscopy. By this analysis, immunoreactivity of $p27^{BBP/eIF6}$ was always found to be associated with the residual thick filaments of the nuclear matrix (Fig. 4 F). Taken together these data show that in the nucleolus and in the nucleus a relevant part of $p27^{BBP/eIF6}$ is tightly associated with the nuclear matrix.

Topographical Relationships of $p27^{BBP/eIF6}$ and β4 at Hemidesmosomes in Epithelial Cells

In epithelial cells containing the β4 integrin, the pattern of immunoreactivity of $p27^{BBP/eIF6}$ was slightly different and is briefly described using the epithelial cell line 804G clone A. This cell line contains human β4 integrin, clustered in rosettes of hemidesmosomes (Spinardi et al., 1993). As a result, when stained with antibodies against β4, these cells exhibit a typical Swiss cheeselike pattern in which intense β4 staining surrounds cytoplasmic areas devoid of integrin (Fig. 5, A and D). Confocal laser scanning microscopy analysis in the horizontal section (x, y) of $p27^{BBP/eIF6}$ immunolocalization in these cells clearly showed a cytoplasmic staining partially superimposable to the one for β4 integrin (Fig. 5, A and D, β4; B and C, $p27^{BBP/eIF6}$; E, β4–$p27^{BBP/eIF6}$). Most importantly, in the vertical (x, z) and horizontal (x, y) sections, both β4 and $p27^{BBP/eIF6}$ stainings were excluded from the small circular areas forming the holes of the Swiss cheeselike pattern (Fig. 5, A′ and D; B′ and C). However, staining with the labeled actin-binding drug, phalloidin, showed that these holes contained other cytoskeletal components such as actin and actin-binding proteins (data not shown; Spinardi, L., manuscript in preparation). These data suggest that in epithelial cells that require β4 to form hemidesmosomes, $p27^{BBP/eIF6}$ can be specifically recruited in the intermediate filament's cytoskeleton converging on these adhesion structures.

To extend these observations, the presence of $p27^{BBP/eIF6}$ was analyzed by immunoelectron microscopy on cryosections of human amnion, a tissue that contains hemidesmosomes clustered at the basal cell surface. Consistent with the pattern observed in the 804G clone A cells, $p27^{BBP/eIF6}$ was detected at the level of inner plaque of the hemidesmosome, where it seemed associated with a thin filament network (Behzad, 1995) running between the intermediate filaments and the hemidesmosomal dense plaque (5-nm gold beads; Fig. 5, F and H, arrowheads). A specific immunolabeling was also noticed in the cytoplasm associated with filamentous structures (e.g., the area indicated by the arrow in Fig. 5, G and H), and also at the inner face of desmosomes (Fig. 5 I). In agreement with the association with the intermediate filament cytoskeleton, $p27^{BBP/eIF6}$ immunolocalization was resistant to high salt extraction (not shown). However, the $p27^{BBP/eIF6}$ positive structures (5-nm gold beads) were within intermediate filament bundles, as shown by a double staining with antikeratin antibodies (15-nm gold beads; Fig. 5, G and H, arrows).

$p27^{BBP/eIF6}$ Is Essential for Yeast Cell Viability

To gain more insights into $p27^{BBP/eIF6}$ function, several approaches were taken, but our efforts to manipulate the levels of $p27^{BBP/eIF6}$ in mammalian cell lines were not successful. Briefly, the expression of $p27^{BBP/eIF6}$ antisense mRNA in NIH/3T3 cells led only to a small decrease of protein levels and established clones could not be derived (Sanvito, F., unpublished observations). Furthermore, transient expression of several mutated constructs in COS cells led in some cases to accumulation of $p27^{BBP/eIF6}$ either in the nucleus or in the cytoplasm, and was toxic to the cells (Sanvito, F., unpublished observations). These observations, together with the nucleolar localization and the fact that the protein is conserved from yeast to humans (Biffo et al., 1997; Si et al., 1997), might suggest a conserved function for this protein, which should be independent of β4 integrin (*S. cerevisiae* does not have β4 homologues). The possibility that $p27^{BBP/eIF6}$ has an ancestral function is further supported by the finding that putative genes encoding peptides homologous to human $p27^{BBP/eIF6}$ are present in the genome of different *Archibacteria* and are also found in plants (Fig. 6).

The analysis of the conserved amino acid sequences does not provide any insight into $p27^{BBP/eIF6}$ function. However, the fact that *S. cerevisiae* contains a $p27^{BBP/eIF6}$ homologue, 80% identical to the human protein, allowed

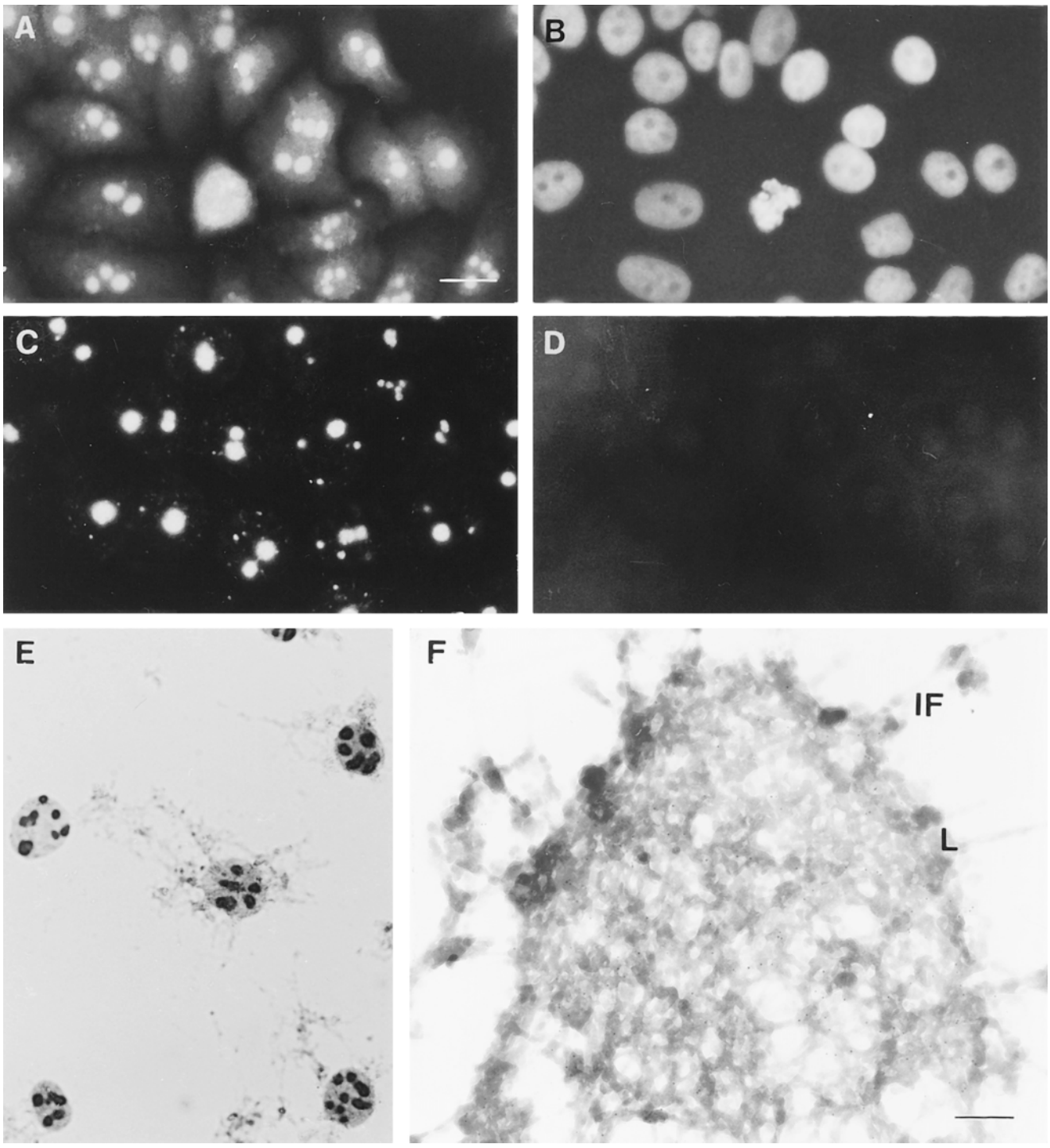

Figure 4. $p27^{BBP/eIF6}$ is associated with the nuclear matrix. FG2 cells were stained for $p27^{BBP/eIF6}$ (A, C, and E) and counterstained with Hoechst dye for nuclear DNA (B and D) before (A and B) or after (C, D, and E) extraction of all soluble proteins to reveal the nuclear matrix/intermediate filament cytoskeleton, according to the procedure of He et al. (1990). B (before) and D (after) show the complete loss of nuclear DNA provided by this treatment. In contrast, A (before) and C (after) show that a conspicuous part of $p27^{BBP/eIF6}$ is retained in the nucleolus. E shows a $p27^{BBP/eIF6}$ immunoperoxidase staining of cells, after extraction. Note that although the strongest cytoskeleton associated staining is in the nucleolus (large black dots), a clear residual staining is also visible in the nucleus. (F) To reveal the intimate association of $p27^{BBP/eIF6}$ with the nuclear matrix, immunoelectron microscopy was performed on resinless sections of extracted cells, exposing the polymorphous nuclear matrix filaments (as in Nickerson et al., 1992). Cells were first treated with $p27^{BBP/eIF6}$ antibodies, followed by gold-conjugated antibodies. The electron micrograph shows a nucleus surrounded by the nuclear lamina (L), which anchored the intermediate filaments of the cytoskeleton (IF). The fibers of the nuclear matrix are strongly decorated with 5-nm gold particles indicating the location of $p27^{BBP/eIF6}$. Intense gold labeling was seen throughout the nuclear matrix filaments. Bars: (A–E) 4 μm; (F) 0.15 μm.

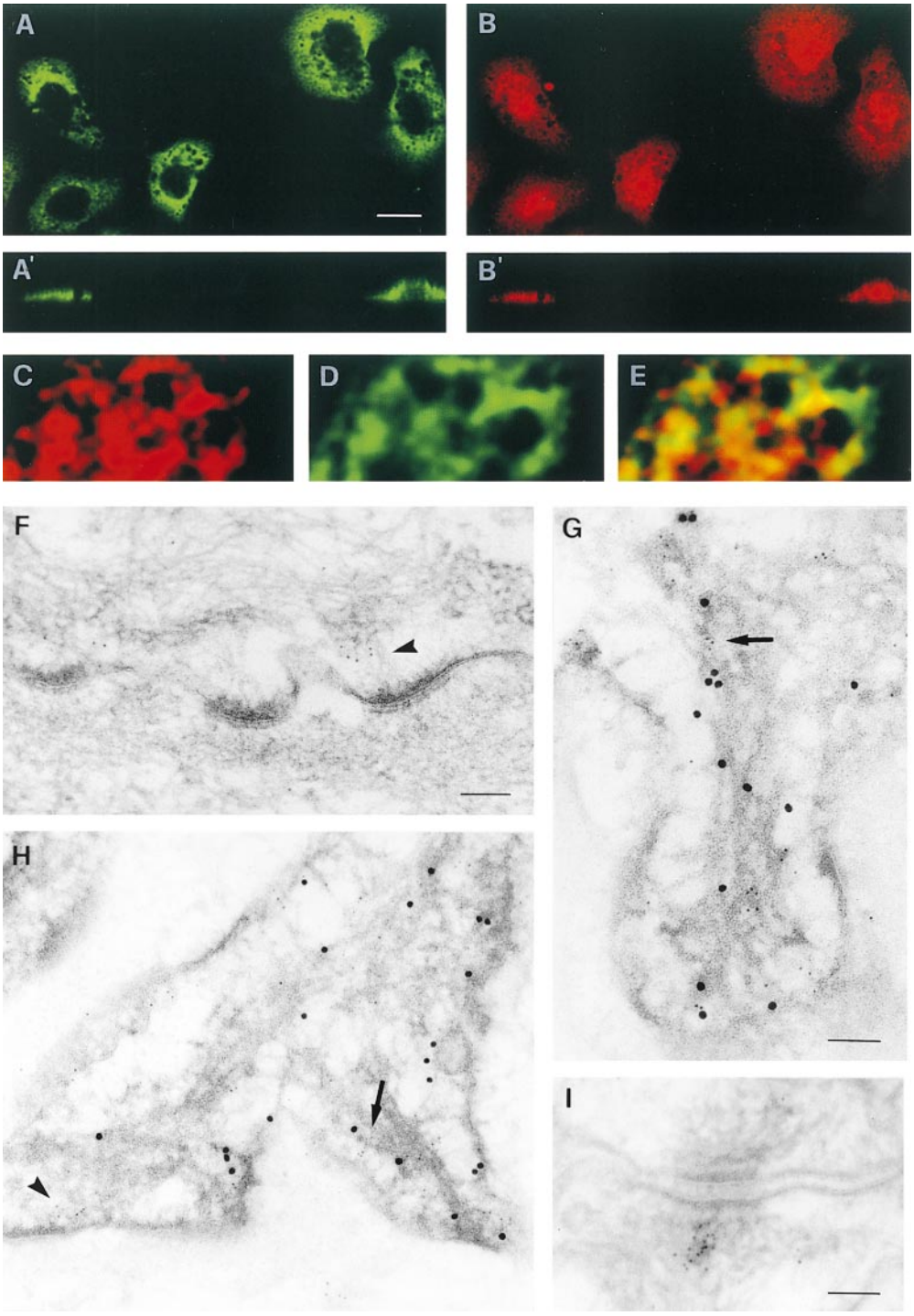

Figure 5. In epithelial cells $p27^{BBP/eIF6}$ distribution is similar to the one of β4 integrin and is present in hemidesmosomes and desmosomes. (A–E) The 804G clone A cell line that expresses human β4 integrin and forms hemidesmosomes in vitro was double-labeled for β4 integrin (A, A′, and D) and $p27^{BBP/eIF6}$ (B, B′, and C), and the results were analyzed in the confocal microscope (E). In horizontal sections (x, y), β4 integrin staining is concentrated in the Swiss cheese pattern formed by hemidesmosome rosettes (A and D). The labeling generated by the $p27^{BBP/eIF6}$ antiserum yields a pattern similar and superimposable to that of β4 (B and C). In vertical sections (x, z) part of $p27^{BBP/eIF6}$ is observed at the basal surface of epithelial cells, where β4 is localized. Note that both β4 and $p27^{BBP/eIF6}$ stainings are excluded from the small circular areas characterizing the Swiss cheese pattern (A′ and B′). Bar, 10 μm. (F–I) Electron microscopy studies were performed on ultracryosections of human amnion immunolabeled with $p27^{BBP/eIF6}$ antiserum (F and I) or double-immunolabeled with both anticytokeratins (15-nm gold beads) and $p27^{BBP/eIF6}$ antiserum (5-nm gold beads) (G and H). The basal cytoplasm of amnion epithelial cells contains a large number of hemidesmosomes, especially in the distal portions of basal cell foot processes. As shown in F and H, $p27^{BBP/eIF6}$ is localized in the innermost plaque of hemidesmosomes (arrowheads) in a region composed of a discrete network of thin filaments between the dense plaque and the intermediate filaments. $p27^{BBP/eIF6}$ immunolabeling is also detected throughout the cytoplasm associated with thin filaments, which are adjacent to intermediate filaments, stained with anticytokeratin (G and H, arrows). $p27^{BBP/eIF6}$ is also present in the cytoskeletal filament network that converges upon desmosomes (I). Bars, 0.125 μm (F); 0.1 μm (G and H); and 0.08 μm (I).

us to analyze the functional role of the protein in the yeast model. The yeast protein is encoded by a single copy gene, which we called *IIH1*. We disrupted one chromosomal copy of the *IIH1* gene in a diploid strain (see Materials and Methods), followed by sporulation of the obtained *IIH1/iih1*Δ heterozygous strain. Tetrad dissection and analysis showed that all tetrads contained only two viable spores (Fig. 7), none of which carried the disruption marker *KanMX4*, indicating that deletion of *IIH1* was lethal. Spores carrying the *iih1*Δ allele were able to germinate, but arrested cell division either in the first or the second cell cycle.

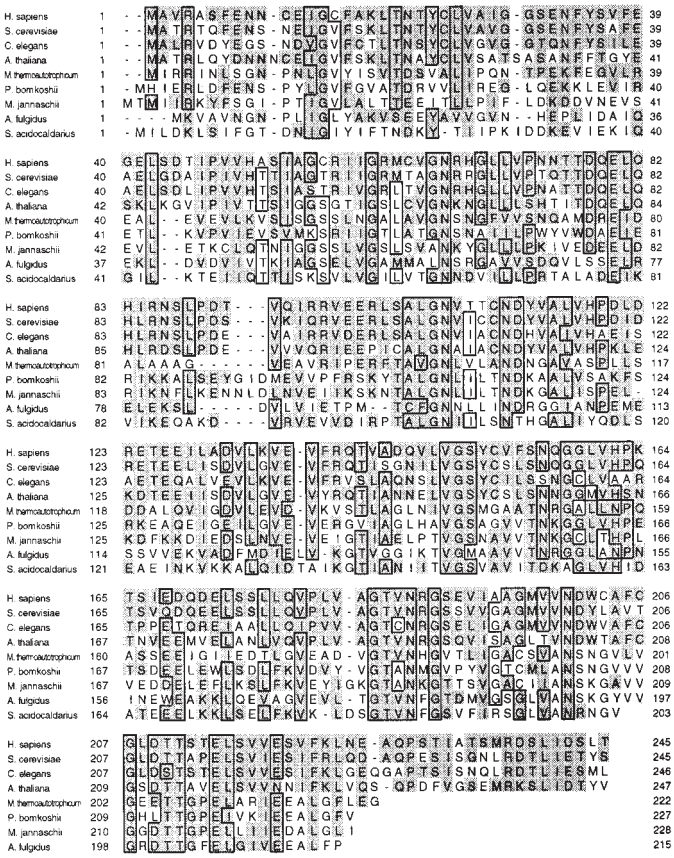

Figure 6. p27$^{BBP/eIF6}$ homologues are present in *Archibacteria.* (Left) alignment of the p27$^{BBP/eIF6}$ protein from various species (human, Y11435; *S. cerevisiae*, Z49919; *C. elegans*, Z99709; *A. thaliana*, AC003000; the *Archibacteria M. jannaschii*, U67463; *S. acidocaldarius*, P38619; *M. thermoautotrophicum*, AE000920; *P. bomkoshii*, AB009481; and *A. fulgidus*, AE000961) obtained with the CLUSTAL W algorithm (for details see Materials and Methods). Identical amino acids are boxed, and homology regions are shadowed. (Right) Phylogenetic tree of the p27$^{BBP/eIF6}$ protein obtained with the GROWTREE program.

We asked whether the human protein could rescue the lethality caused by deletion of the *IIH1* gene. For this purpose, we constructed fusion genes where the yeast or the human p27$^{BBP/eIF6}$ coding sequences were expressed under control of the yeast galactose inducible *GAL1-10* promoter. These fusions were integrated in either single or multiple copies at the yeast *URA3* locus of *IIH1/iih1*Δ heterozygous diploid strains. Subsequently, these integrated fusions underwent induced sporulation to analyze viability of their meiotic segregants under galactose-induced conditions. As shown in Fig. 7, most tetrads derived from any of these diploid strains contained either three or four viable spores, as expected if expression of human p27$^{BBP/eIF6}$ (Hsp27$^{BBP/eIF6}$) was able to rescue the lethality caused by the *iih1*Δ allele. These data indicate that human and yeast

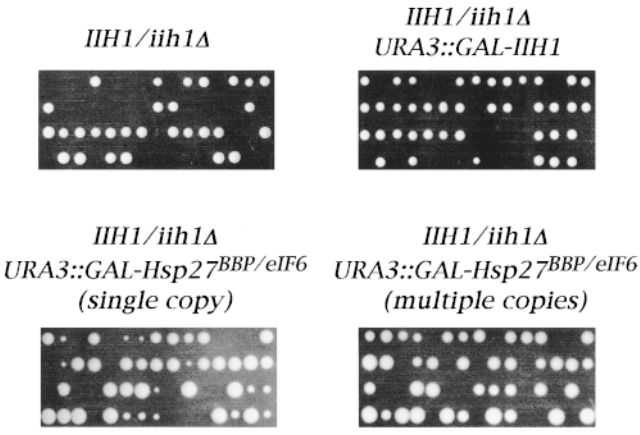

Figure 7. Deletion of the yeast IIH gene results in cell lethality, which can be rescued by expression of its human counterpart. Diploid yeast strains ySP478, ySP650, ySP653 and ySP652, with the indicated genotypes (see text and Materials and Methods) were allowed to sporulate, followed by tetrad dissection on galactose containing medium, and incubation at 28°C. The four spores from each tetrad are aligned vertically.

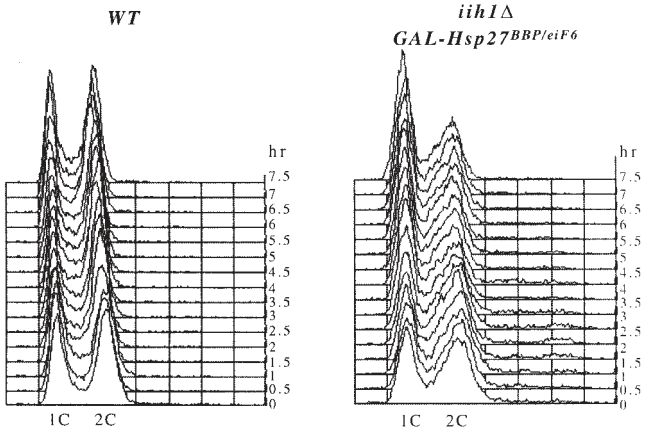

Figure 8. p27$^{BBP/eIF6}$ depletion causes accumulation of G1 cells. Cell cultures of strains W303 (WT) and ySP664 (*iih1*Δ *GAL-Hsp27*$^{BBP/eIF6}$), logarithmically growing in galactose-containing medium, were transferred to glucose-containing medium at time 0. Samples for FACS® analysis were taken at the indicated times.

p27$^{BBP/eIF6}$ share a common function. However, expression of human p27$^{BBP/eIF6}$ seems to complement the defect less efficiently than its yeast counterpart; as indicated by the slower growth of the clones derived from spores expressing a single copy of the human gene and the *iih1*Δ allele (Fig. 7). This might be due to inefficient translation of the human mRNA gene in yeast (CAI-S.c. = 0.076); consistently with this hypothesis, the slow growth phenotype was substantially abolished when multiple copies of the *GAL-Hsp27*$^{BBP/eIF6}$ fusion were integrated at the *ura3* locus (Fig. 7).

Depletion of p27$^{BBP/eIF6}$ Causes Accumulation of G1 Cells

To study the function of p27$^{BBP/eIF6}$ in yeast cells, we characterized the phenotype caused by its depletion. For this purpose, wild-type and *iih1*Δ cells, carrying either the *GAL-IIH1* or the *GAL-Hsp27*$^{BBP/eIF6}$ fusion and logarithmically growing in galactose, were transferred to glucose-containing medium, to switch off the *GAL* promoter. The switch to a glucose-containing medium resulted in the progressive loss of the p27$^{BBP/eIF6}$ protein (not shown). Since the shut-off of the *GAL-Hsp27*$^{BBP/eIF6}$ fusion caused a much quicker arrest of cell division than that of the *GAL-IIH1* fusion, we used the *GAL-Hsp27*$^{BBP/eIF6}$ fusion-expressing strain for all the described depletion experiments. As shown by the FACS® profiles in Fig. 8, yeast cells depleted of p27$^{BBP/eIF6}$, progressively stopped growing and accumulated as G1 cells with 1C DNA content. This phenotype is consistent with a role of p27$^{BBP/eIF6}$ in protein synthesis since yeast cells need to grow in cell mass and reach a critical size before they can enter the S phase.

p27$^{BBP/eIF6}$ Depletion Correlates with the Loss of Free 60S Ribosomal Subunit

The arrest of p27$^{BBP/eIF6}$ depleted cells in G1, the fact that p27$^{BBP/eIF6}$ has been independently identified as a putative translation initiation factor (Si et al., 1997) and our observation that p27$^{BBP/eIF6}$ is detected in the nucleolus of all cell lines, suggested that this protein might be involved in protein synthesis and/or ribosome assembly. To understand the relevance of p27$^{BBP/eIF6}$ in one of these processes in yeast, the polysome profiles of wild-type– and p27$^{BBP/eIF6}$–depleted cells were analyzed. For this purpose, wild-type and *iih*Δ strains carrying the *GAL-Hsp27*$^{BBP/eIF6}$ were grown in galactose-containing medium, and then shifted to glucose-containing medium to switch off the *GAL* promoter. As a control, a strain where the *iih1*Δ allele lethality was rescued by the *GAL-IIH1* fusion was also used.

As shown in Fig. 9, the ribosomal profiles of *wt* and *iih1*Δ *GAL-IIH1* strains were very similar at time 0, whereas *iih1*Δ *GAL-Hsp27*$^{BBP/eIF6}$ cells, consistently with their slow growth phenotype, already showed a marked decrease in the amount of both the 60S subunit and the polysome fraction at the same time point. In contrast, the levels of the free 40S subunit seemed unaffected or slightly increased. This phenotype was even more dramatic 6 h after shifting to the glucose-containing medium of *iih1*Δ *GAL-Hsp27*$^{BBP/eIF6}$ cells (Fig. 9). Furthermore, an accumulation of half-mer polysomes (i.e., 80S + 60S) was detectable under these conditions. These data suggest that

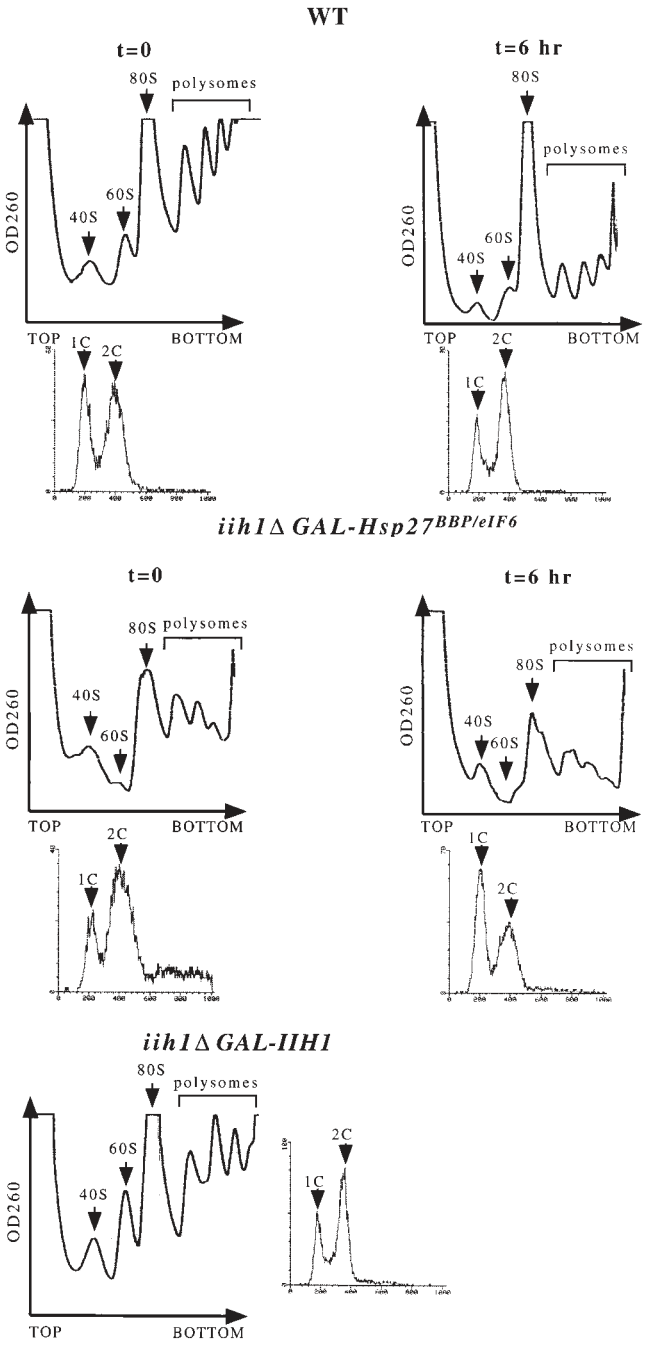

Figure 9. p27$^{BBP/eIF6}$ depletion results in a reduced level of free 60S ribosomal subunit. Cell cultures of strains W303 (WT) and ySP664 (*iih1*Δ *GAL-Hsp27*$^{BBP/eIF6}$), logarithmically growing in galactose-containing medium, were transferred to glucose-containing medium at time 0. Samples for polyribosome preparation and polysome analysis were taken at time 0 and 6 h after shifted to glucose-containing medium. Polysome profiles after the sucrose gradient centrifugation of yeast extracts (see Materials and Methods) are shown in the top, and FACS® profiles of the corresponding cell cultures are shown in the bottom. As a control, the same procedure was applied to strain ySP661 (*iih1*Δ *GAL-IIH1*), whose polysome profile (left) and FACS® profile (right) at time 0 are shown in the bottom.

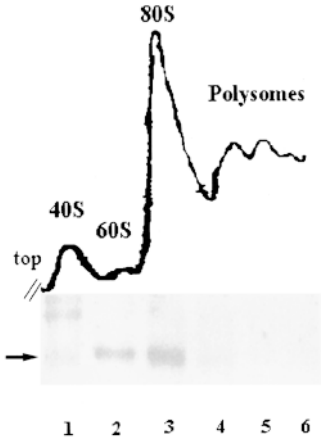

Figure 10. $p27^{BBP/eIF6}$ cosediments with 60S and 80S ribosomal subunits. Fractions collected after the sucrose gradient centrifugation (top) of extracts from strain ySP-664 (*iih1*Δ *GAL-Hsp27*$^{BBP/eIF6}$), logarithmically growing in galactose-containing medium, were precipitated by TCA, and equal amounts of protein extracts were run on 12% acrylamide gels, transferred on immobilon-P membranes and probed with the anti–$p27^{BBP/eIF6}$ antiserum, followed by the ECL detection method (bottom). Note that $p27^{BBP/eIF6}$ (arrow) is highly enriched in the free 60S and 80S fractions, but clearly absent from the polysome fraction. The high molecular weight band in lane 1 is a nonspecific product recognized by secondary antibodies.

$p27^{BBP/eIF6}$ might have a primary function in the correct assembly of the 60S ribosomal subunit in yeast.

Cofractionation of human $p27^{BBP/eIF6}$ in yeast cells was analyzed in parallel. For this end, fractions from the ribosomal gradients were precipitated with TCA and analyzed by Western blot using antibodies against the human protein. As shown in Fig. 10, $p27^{BBP/eIF6}$ was detected in the 80S and in the free 60S fractions, but absent from polysomes.

Discussion

$p27^{BBP/eIF6}$ was simultaneously identified by two laboratories using two different approaches. It was isolated in our laboratory as a cytoplasmic interactor of the β4 integrin subunit, and we have shown that it can specifically bind the cytodomain of β4 in vitro (Biffo et al., 1997). However, the discovery of $p27^{BBP/eIF6}$ homologues in organisms that do not contain β4 indicated that this protein might have a function independent of β4. Along this line, $p27^{BBP/eIF6}$ was independently identified by Si et al. (1997) as a putative translation initiation factor, able to inhibit the association between the 60S and the 40S ribosomal subunits.

In this study, we have shown that although in epithelial cells $p27^{BBP/eIF6}$ is coherent with β4 at hemidesmosomes, its association with the cytoskeleton is not a unique feature of epithelial cells. Indeed the protein is in the nuclear matrix of all growing cells. Consistently with its conserved nucleolar expression pattern and sequence, $p27^{BBP/eIF6}$ is necessary for growth in yeast cells where its loss correlates with a reduced level of the free 60S ribosomal subunit. The in vivo findings were unexpected because they were consistent with a role of $p27^{BBP/eIF6}$ in ribosomal biogenesis rather than in mRNA translation. In addition, the association of $p27^{BBP/eIF6}$ with the nuclear matrix suggested that this process was linked to the nuclear cytoskeleton. The ability of the human protein to complement yeast mutation further suggested a conserved function for $p27^{BBP/eIF6}$.

An Evolutionarily Conserved Function for $p27^{BBP/eIF6}$ in 60S Metabolism

Database analysis indicates that $p27^{BBP/eIF6}$ is a very ancient, evolutionarily conserved protein. It is striking to note that the homology is not restricted to a particular domain of the protein, and that even the length of the protein is constant among different species (246 amino acids in *C. elegans*; 245 in humans, fly, yeast, and *A. thaliana*; and 215–222 in different *Archibacteria*). These data suggest that $p27^{BBP/eIF6}$ may have a critical and conserved function. Indeed, we have shown that the deletion of the *S. cerevisiae IIH1* gene, encoding the $p27^{BBP/eIF6}$ homologue, is lethal to yeast cells, and that the human protein can complement the yeast-null mutation. Some lines of evidence suggest that also in mammalian cells, $p27^{BBP/eIF6}$ may be required for growth because of the following: (a) the inability to produce stable $p27^{BBP/eIF6}$ mRNA antisense expressing mammalian cells (not shown); (b) the ubiquitous $p27^{BBP/eIF6}$ expression in all immortalized cell lines so far analyzed; (c) and the presence of a single $p27^{BBP/eIF6}$ gene in the human genome (Sanvito et al., 1998). The generation of $p27^{BBP/eIF6}$-null mice will help to understand whether $p27^{BBP/eIF6}$ is also necessary for growth in higher vertebrates. Unfortunately, extensive sequence analysis did not yield significant clues to understand $p27^{BBP/eIF6}$ function.

To gain some insights into this problem, we used two complementary approaches: the depletion of $p27^{BBP/eIF6}$ in the genetically manipulable yeast model, and the study of its topographical localization and biochemical properties in mammalian cell lines and tissues. Yeast cells depleted of $p27^{BBP/eIF6}$ are progressively arrested in G1, a phenotype consistent with a defect in either protein synthesis or ribosomal biogenesis. This fact, and the localization of $p27^{BBP/eIF6}$ in nucleoli prompted us to analyze the effect of its depletion on the polysome profile. These experiments provide useful information about how $p27^{BBP/eIF6}$, based on its in vitro ribosomal anti-association activity, could be a translation initiation factor (Si et al., 1997). Polysome profiles of $p27^{BBP/eIF6}$-depleted yeast cells showed a dramatic reduction in the peak of free 60S subunits and the appearance of half-mer polysomes. Similar polysome profiles have been observed for mutants defective in ribosomal proteins of the 60S ribosomal subunit (Moritz et al., 1991; Deshmukh et al., 1993; Vilardell and Warner, 1997), or for components involved in pre-rRNA processing and 60S ribosomal subunit assembly (Ripmaster et al., 1992; Sun and Woolford, 1994; Hong et al., 1997; Weaver et al., 1997; Zanchin et al., 1997; Kressler et al., 1998). Thus, the primary function of $p27^{BBP/eIF6}$ in yeast is likely related to the 60S ribosomal subunit metabolism.

Polysome profiles of yeast cells, defective in translation initiation factor proteins, are generally characterized by the reduction of the rate of polysomes accompanied by the gradual accumulation of both the free 40S and 60S subunits. Therefore, the polysome profile of $p27^{BBP/eIF6}$-depleted yeast cells does not support its primary function as a translation initiation factor. However, on the basis of the in vitro data of Si et al. (1997), and in view of the presence of $p27^{BBP/eIF6}$ also in the cytoplasm of some human cells, the possibility that this protein might have a function also as a cytosolic initiation factor cannot be ruled out, as such ac-

tivity could be masked by the predominant defect in 60S metabolism.

The polysome profile does not enlighten the precise role played by p27$^{BBP/eIF6}$ in 60S metabolism. The protein may be necessary for ribosome assembly/transport, or may act as a structural ribosomal protein. On the basis of the available data, this last possibility is less likely to be true. In fact, the amount of p27$^{BBP/eIF6}$ sedimenting with the ribosomal fraction in several cell lines represents only a minor fraction of the total p27$^{BBP/eIF6}$ content. Furthermore, no p27$^{BBP/eIF6}$ was detected in the polysome fraction.

p27$^{BBP/eIF6}$ accumulates in the nucleolus of all the analyzed cell lines, where its pattern follows nucleolar evolution (redistribution at mitosis, when the nucleolar organizing region disappears, and redistribution after actinomycin D treatment). Since the nucleolus is the site where ribosomal subunits are assembled, it seems plausible to speculate that p27$^{BBP/eIF6}$ might be involved in 60S ribosomal biogenesis. The process of ribosome biogenesis is complex and involves several factors (for review see Woolford and Warner, 1991; Eichler and Craig, 1994) including proteins with diverse functions such as RNA helicases, transcription factors, and nucleases. Further studies will address the precise role that p27$^{BBP/eIF6}$ might play in this process.

Finally, it is possible that p27$^{BBP/eIF6}$ may be involved in the transport of the 60S subunit from the nucleus to the cytoplasm. To date, very little is known about this process (for review see Shaw and Jordan, 1995), and only a few nucleolar proteins have been found to shuttle between the nucleolus and the cytoplasm. In this context, three observations are particularly intriguing: (a) the presence of p27$^{BBP/eIF6}$ both in a soluble pool and in a cytoskeletal bound compartment; (b) the existence of trace amounts of soluble cytoplasmic p27$^{BBP/eIF6}$ in all cells; and (c) the ability of p27$^{BBP/eIF6}$ to bind also the mature 60S subunit (Si et al., 1997).

It is also worth noting that the nucleolar localization of p27$^{BBP/eIF6}$ is observed in the absence of a consensus nuclear localization signal. Therefore, either p27$^{BBP/eIF6}$ carries an unknown sequence for nuclear targeting or it is targeted into the nucleus by binding an additional factor in the cytoplasm. The second hypothesis is supported by the fact that even in its most soluble form, p27$^{BBP/eIF6}$ partitions in gel filtration as a high molecular weight complex (unpublished observation). The molecular dissection of this high molecular weight complex may shed light on the mechanism by which p27$^{BBP/eIF6}$ is transported to the nucleus.

p27$^{BBP/eIF6}$ in the Nuclear Matrix/Intermediate Filaments Fraction

Our study shows that a relevant fraction of p27$^{BBP/eIF6}$ is highly insoluble in vivo and is associated both with the nuclear matrix and with the intermediate filament pool. In the cytoplasm, electron microscopy studies have detected p27$^{BBP/eIF6}$ on thin cytoplasmic filaments of unknown composition that are spatially separated from the classical keratin intermediate filaments, and converge both upon hemidesmosomes and desmosomes. To our knowledge, beside keratins, only another intermediate filament associated protein, IFAP300, has been described both in hemidesmosomes and desmosomes (Skalli et al., 1994). In this context, it is interesting to note that a recent thorough electron microscopy analysis of human hemidesmosomes has shown the presence of a novel filamentous structure in the proximity of the inner plaque of the hemidesmosome (Behzad et al., 1995).

Nuclear matrix consists of both thick polymorphous filaments and of thin filaments known as core filaments (He et al., 1990). In the nucleus, p27$^{BBP/eIF6}$ is associated with polymorphous thick filaments, and is absent from the core filaments. This observation is fully consistent with the notion that core filaments may be formed by nuclear RNA, and that p27$^{BBP/eIF6}$ distribution is resistant to RNase digestion (He et al., 1990). The localization of p27$^{BBP/eIF6}$ in the nuclear matrix is of extreme interest in the context of ribosome biogenesis. Our data provide an intriguing link between the nuclear cytoskeleton and the process of ribosome assembly.

In recent years growing evidence has indicated that most nuclear and cytoplasmic processes including transcription, DNA replication, and protein synthesis are spatially organized in association with the cytoskeleton. The combined roles of p27$^{BBP/eIF6}$ protein in 60S assembly, its association with the cytoskeleton, and its ability to bind β4 integrin (Biffo et al., 1997) and the mature 60S ribosome subunit (Si et al., 1997) belong to an integrated view of cell regulation that encompasses structure as well as biochemical processes (Chicurel et al., 1998).

p27$^{BBP/eIF6}$ and β4 Integrin

We have previously shown that p27$^{BBP/eIF6}$ binds specifically to the cytodomain of β4 integrin in vitro and in yeast (Biffo et al., 1997). Our previous data, and specifically the association of p27$^{BBP/eIF6}$ with keratin intermediate filaments, strongly suggested that this interaction could occur also in vivo and be necessary for targeting β4 to hemidesmosomes and intermediate filaments. Since intermediate filament-associated proteins can be solubilized only upon SDS treatment, rendering the maintenance of biochemical interactions impossible, an association between β4 and p27$^{BBP/eIF6}$ in tissues could not be proved. We now provide two further elements suggesting that p27$^{BBP/eIF6}$ is functionally associated to the β4 integrin in vivo: (a) its peculiar Swiss cheese distribution is superimposable to that of β4 in cells that form hemidesmosomes; and (b) the presence of the protein, in vivo, in hemidesmosomes of the human amnion. Further experiments are needed to clarify the functional significance of β4–p27$^{BBP/eIF6}$ interaction, and specifically whether p27$^{BBP/eIF6}$ may direct β4 to hemidesmosomes. Alternatively, as it has been recently suggested, on the basis of in vitro evidence and yeast two-hybrid assays, the crucial step in targeting β4 to hemidesmosomes is the interaction with the large intermediate filament-associated protein, HD-1 (Niessen et al., 1997; Rezniczeck et al., 1998). If this is the case also in vivo, then the role of p27$^{BBP/eIF6}$ binding to β4 may be related to a nonstructural function of β4 integrin, similar to that shown in the case of the recruitment of shc and grb2 (Mainiero et al., 1995) or of PI3 kinase (Shaw et al., 1997).

In the absence of further evidence, we may reasonably suggest that p27$^{BBP/eIF6}$ has an evolutionarily conserved

function linked to 60S ribosome biogenesis, and one acquired during evolution in epithelial cells containing β4 integrin. At least one precedent of a protein with a dual function acquired during evolution, i.e., β-catenin/armadillo, has already been reported. This remarkable protein can be found both at sites of cell–cell adhesion in connection to cadherins and in the nucleus where it can signal in conjunction with LEF-1 (for review see Willert and Nusse, 1998).

We thank R. Ochs for the kind gift of human antibodies directed against fibrillarin, F. Giancotti for permission to use clone A of the 804G cell line, and J. Nickerson for advice on nuclear matrix preparation. We are indebted to N. Offenhaeuser for useful suggestion and criticism throughout this work, to A. Hinnebusch and M. Foiani for useful suggestions, G. Serini for having pushed us to perform some experiments, E. Bianchi for her criticism, and E. Rizzo for the preparation and purification of the recombinant $p27^{BBP}$ protein used in the preadsorption experiments and the experiments with actinomycin D.

The financial support of Telethon-Italy (grant 762 and E.712) is gratefully acknowledged. The work was supported also by Associazione Italiana per la Ricerca sul Cancro, Giovanni Armenise-Harvard Foundation, and MURST to P.C. Marchisio, and by CNR Target Project on Biotechnology Grant CT.97.01180.PF49(F).

Received for publication 15 September 1998 and in revised form 14 January 1999.

References

Behzad, F., C.J. Jones, S. Ball, T. Alvares, and J.D. Aplin. 1995. Studies of hemidesmosomes in human amnion: the use of a detergent extraction protocol for compositional and ultrastructural analysis and preparation of a hemidesmosome-enriched fraction from tissue. *Acta Anat.* 152:170–184.

Biffo, S., F. Sanvito, S. Costa, L. Preve, R. Pignatelli, L. Spinardi, and P.C. Marchisio. 1997. Isolation of a novel beta4 integrin-binding protein (p27(BBP)) highly expressed in epithelial cells. *J. Biol. Chem.* 272:30314–30321.

Boukamp, P., R.T. Petrussevska, D. Breitkreutz, J. Hornung, A. Markham, and N.E. Fusenig. 1988. Normal keratinization in a spontaneously immortalized aneuploid human keratinocyte cell line. *J. Cell Biol.* 106:761–771.

Chicurel, M.E., R.H. Singer, C.J. Meyer, and D.E. Ingber. 1998a. Integrin binding and mechanical tension induce movement of mRNA and ribosomes to focal adhesions. *Nature.* 392:730–733.

Chicurel, M.E., C.S. Chen, and D.E. Ingber. 1998b. Cellular control lies in the balance of forces. *Curr. Opin. Cell Biol.* 10:232–239.

Cho, S.H., J.J. Cho, I.I. Kim, H. Vliagoftis, D.D. Metcalfe, and C.K. Oh. 1998. Identification and characterization of the inducible murine mast cell gene, imc-415. *Biochem. Biophys. Res. Commun.* 9:123–127.

Clark, E.A., and J.S. Brugge. 1995. Integrins and signal transduction pathways: the road taken. *Science.* 268:233–239.

Deshmukh, M., Y.F. Tsay, A.G. Paulovich, and J.L. Woolford, Jr. 1993. Yeast ribosomal protein L1 is required for the stability of newly synthesized 5S rRNA and the assembly of 60S ribosomal subunits. *Mol. Cell. Biol.* 13:2835–2845.

Dowling, J., Q.C. Qu, and E. Fuchs. 1996. Beta4 integrin is required for hemidesmosome formation, cell adhesion, and cell survival. *J. Cell Biol.* 134: 559–572.

Earnshaw, W.C., and R.L. Bernat. 1991. Chromosomal passengers: toward an integrated view of mitosis. *Chromosoma.* 100:139–146.

Eichler, D.C., and N. Craig. 1994. Processing of eukaryotic ribosomal RNA. *Prog. Nuc. Acid Res. Mol. Biol.* 49:197–239.

Foiani, M., A.M. Cigan, C.J. Paddon, S. Harashima, and A.G. Hinnebusch. 1991. GCD2, a translational repressor of the GCN4 gene, has a general function in the initiation of protein synthesis in *Saccharomyces cerevisiae. Mol. Cell Biol.* 11:3203–3216.

Giancotti, F.G. 1996. Signal transduction by the alpha 6 beta 4 integrin: charting the path between laminin binding and nuclear events. *J. Cell Sci.* 109:1165–1172.

Giancotti, F.G. 1997. Integrin signaling: specificity and control of cell survival and cell cycle progression. *Curr. Opin. Cell Biol.* 9:691–700.

Gietz, R.D., and A. Sugino. 1988. New yeast–*Escherichia coli* shuttle vectors constructed with in vitro mutagenized yeast genes lacking six-base pair restriction sites. *Gene.* 74:527–534.

Green, S., I. Issemann, and E. Sheer. 1988. A versatile in vivo and in vitro eukaryotic expression vector for protein engineering. *Nucleic Acids Res.* 16: 369.

He, D.C., J.A. Nickerson, and S. Penman. 1990. Core filaments of the nuclear matrix. *J. Cell Biol.* 110:569–580.

Hong, B., J.S. Brockenbrough, P. Wu, and J.P. Aris. 1997. Nop2p is required for pre-rRNA processing and 60S ribosome subunit synthesis in yeast. *Mol. Cell. Biol.* 17:378–388.

Howe, A., A.E. Aplin, S.K. Alahari, and R.L. Juliano. 1998. Integrin signaling and cell growth control. *Curr. Opin. Cell Biol.* 10:220–231.

Hynes, R.O. 1992. Integrins: versatility, modulation, and signaling in cell adhesion. *Cell.* 69:11–25.

Kajiji, S., R.N. Tamura, and V. Quaranta. 1989. A novel integrin (alpha E beta 4) from human epithelial cells suggests a fourth family of integrin adhesion receptors. *EMBO (Eur. Mol. Biol. Organ.) J.* 8:673–680.

Kressler, D., J. de la Cruz, M. Rojo, and P. Linder. 1998. Dbp6p is an essential putative ATP-dependent RNA helicase required for 60S-ribosomal-subunit assembly in *Saccharomyces cerevisiae. Mol. Cell. Biol.* 18:1855–1865.

Laemmli, U.K. 1970. Cleavage of structural proteins during the assembly of the head of bacteriophage T4. *Nature.* 227:680–685.

Madjar, J.J. 1994. Preparation of ribosomes and ribosomal proteins from cultured cells. *In* Cell Biology: A Laboratory Handbook. Academic Press Inc., Orlando, FL. 657–661.

Mainiero, F., A. Pepe, K.K. Wary, L. Spinardi, M. Mohammadi, J. Schlessinger, and F.G. Giancotti. 1995. Signal transduction by the alpha 6 beta 4 integrin: distinct beta 4 subunit sites mediate recruitment of Shc/Grb2 and association with the cytoskeleton of hemidesmosomes. *EMBO (Eur. Mol. Biol. Organ.) J.* 14:4470–4481.

Marchisio, P.C., S. Bondanza, O. Cremona, R. Cancedda, and M. De Luca. 1991. Polarized expression of integrin receptors (α6β4, α2β1, α3β1, and αvβ5) and their relationship with the cytoskeleton and basement membrane matrix in cultured human keratinocytes. *J. Cell Biol.* 112:761–773.

Nickerson, J.A., G. Krockmalnic, K.M. Wan, C.D. Turner, and S. Penman. 1992. A normally masked nuclear matrix antigen that appears at mitosis on cytoskeleton filaments adjoining chromosomes, centrioles, and midbodies. *J. Cell Biol.* 116:977–987.

Nickerson, J.A., G. Krockmalnic, and S. Penman. 1994. Isolation and visualization of the nuclear matrix, the nonchromatin structure of the nucleus. *In* Cell Biology: A Laboratory Handbook. Academic Press Inc., Orlando, FL. 622–627.

Niessen, C.M., E.H. Hulsman, L.C. Oomen, I. Kuikman, and A. Sonnenberg. 1997. A minimal region on the integrin beta4 subunit that is critical to its localization in hemidesmosomes regulates the distribution of HD1/plectin in COS-7 cells. *J. Cell Sci.* 110:1705–1716.

Ochs, R.L., and K. Smetana. 1991. Detection of fibrillarin in nucleolar remnants and the nucleolar matrix. *Exp. Cell Res.* 197:183–190.

Rezniczek, G.A., J.M. de Pereda, S. Reipert, and G. Wiche. 1998. Linking integrin alpha6beta4-based cell adhesion to the intermediate filament cytoskeleton: direct interaction between the beta4 subunit and plectin at multiple molecular sites. *J. Cell Biol.* 141:209–225.

Ripmaster, T.L., G.P. Vaughn, and J.L. Woolford, Jr. 1992. DRS1 to DRS7, novel genes required for ribosome assembly and function in *Saccharomyces cerevisiae. Mol. Cell. Biol.* 13:7901–7912.

Rose, M.D., F. Winston, and P. Hieter. 1990. Methods in yeast genetics. Cold Spring Harbor Laboratory, Cold Spring Harbor, NY. 192 pp.

Rouiller, D.G., V. Cirulli, and P.A. Halban. 1990. Differences in aggregation properties and levels of the neural cell adhesion molecule (NCAM) between islet cell types. *Exp. Cell Res.* 191:305–312.

Sambrook, J., E.F. Fritsch, and T. Maniatis. 1989. Molecular Cloning. A Laboratory Manual. Cold Spring Harbor Laboratory, Cold Spring Harbor, NY.

Sanvito, F., G. Arrigo, O. Zuffardi, M. Agnelli, P.C. Marchisio, and S. Biffo. 1998. Localization of p27 beta4 binding protein gene (ITGB4BP) to human chromosome region 20q11.2. *Genomics.* 51:111–112.

Schofer, C., K. Weipoltshammer, M. Almeder, M. Muller, and F. Wachtler. 1996. Redistribution of ribosomal DNA after blocking of transcription induced by actinomycin D. *Chromosome Res.* 4:384–391.

Shaw, L.M., I. Rabinovitz, H.H. Wang, A. Toker, and A.M. Mercurio. 1997. Activation of phosphoinositide 3-OH kinase by the alpha6beta4 integrin promotes carcinoma invasion. *Cell.* 91:949–960.

Shaw, P.J., and E.G. Jordan. 1995. The nucleolus. *Annu. Rev. Cell. Dev. Biol.* 11:93–121.

Si, K., J. Chaudhuri, J. Chevesich, and U. Maitra. 1997. Molecular cloning and functional expression of a human cDNA encoding translation initiation factor 6. *Proc. Natl. Acad. Sci. USA.* 94:14285–14290.

Skalli, O., J.C. Jones, R. Gagescu, and R.D. Goldman. 1994. IFAP 300 is common to desmosomes and hemidesmosomes and is a possible linker of intermediate filaments to these junctions. *J. Cell Biol.* 125:159–170.

Spinardi, L., Y.L. Ren, R. Sanders, and F.G. Giancotti. 1993. The beta 4 subunit cytoplasmic domain mediates the interaction of alpha 6-beta 4 integrin with the cytoskeleton of hemidesmosomes. *Mol. Biol. Cell.* 4:871–884.

Sun, C., and J.L. Woolford, Jr. 1994. The yeast NOP4 gene product is an essential nucleolar protein required for pre-rRNA processing and accumulation of 60S ribosomal subunits. *EMBO (Eur. Mol. Biol. Organ.) J.* 13:3217–3235.

Thompson, J.D., D.G. Higgins, and T.J. Gibson. 1994. CLUSTAL W: improving the sensitivity of progressive multiple sequence alignment through sequence weighting, position-specific gap penalties and weight matrix choice. *Nucleic Acids Res.* 22:4673–4680.

van der Neut, R., P. Krimpenfort, J. Calafat, C.M. Niessen, and A. Sonnenberg. 1996. Epithelial detachment due to absence of hemidesmosomes in integrin

beta 4 null mice. *Nat. Genet.* 13:366–369.

Vidal, F., D. Aberdam, C. Miquel, A.M. Christiano, L. Pulkkinen, J. Uitto, J.P. Ortonne, and G. Meneguzzi. 1995. Integrin beta 4 mutations associated with junctional epidermolysis bullosa with pyloric atresia. *Nat. Genet.* 10:229–234.

Vilardell, J., and J.R. Warner. 1997. Ribosomal protein L32 of *Saccharomyces cerevisiae* influences both the splicing of its own transcript and the processing of rRNA. *Mol. Cell. Biol.* 174:1959–1965.

Villa, A., P. Podini, M.C. Panzeri, H.D. Soling, P. Volpe, and J. Meldolesi. 1993. The endoplasmic-sarcoplasmic reticulum of smooth muscle: immunocytochemistry of vas deferens fibers reveals specialized subcompartments differently equipped for the control of Ca^{2+} homeostasis. *J. Cell Biol.* 121:1041–1051.

Wach, A., A. Brachat, R. Pohlmann, and P. Philippsen. 1994. New heterologous modules for classical or PCR-based gene disruptions in *Saccharomyces cerevisiae. Yeast.* 10:1793–1808.

Weaver, P.L., C. Sun, and T.H. Chang. 1997. Dbp3p, a putative RNA helicase in *Saccharomyces cerevisiae*, is required for efficient pre-rRNA processing predominantly at site A3. *Mol. Cell. Biol.* 17:1354–1365.

Willert, K., and R. Nusse. 1998. Beta-catenin: a key mediator of Wnt signaling. *Curr. Op. Genet. Dev.* 8:95–102.

Zanchin, N.I., P. Roberts, A. De Silva, F. Sherman, and D.S. Goldfarb. 1997. *Saccharomyces cerevisiae* Nip7p is required for efficient 60S ribosome subunit biogenesis. *Mol. Cell. Biol.* 17:5001–5015.